Directional effects on pigment cell precursors in uniaxially stretched mouse embryonic skin

Johan Rott[1], Irwin Phanada[1], Sarah Woolner[1], Oliver Jensen[2], Kerrie Marie[1]

[1]School of Biological Sciences, University of Manchester, Oxford Road, Manchester, UK.
[2]Department of Mathematics, University of Manchester, Oxford Road, Manchester, UK.

Introduction

- In mammalian embryos, **mechanical forces** propagating through **skin tissue** help coordinate its **morphogenesis**.
- **Melanoblasts** (melanocyte precursors) experience these forces as they **migrate** and **proliferate** to colonise the skin:

1. **Tension** in the epidermis caused by rapid embryonic growth[1].
2. **Cell crowding** in the basal layer driving epidermal stratification[2].
3. **Contractile flows** during hair follicle morphogenesis[3].

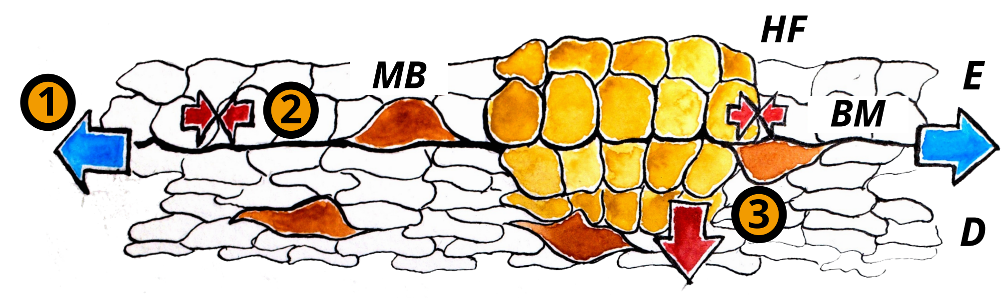

Fig 1: Forces in skin development at mouse embryonic stage E14.5. Arrows show tension (blue) or compression (red). E: epidermis, D: dermis, MB: melanoblast, HF: hair follicle, BM: basement membrane.

Research questions:

- Can mechanical forces cue melanoblast behaviours?
- Do mechanical cues participate in regulating melanocytic cells across health and disease?

Methods

iDct-G;mT: reporter mouse model to visualise melanoblasts in native tissue environment

- Created by crossing **iDct-GFP**[4] and **mTmG**[5] transgenic mice, the **iDct-G;mT** model inducibly expresses **H2B-GFP** in the melanocytic lineage (driven by *Dct* promoter) as well as expressing membrane-targeted **tdTomato** in all cells.
- We assess normal development of the **basal epidermis**. At E13.5, basal cells show **dorsoventral (D/V) elongation**, while melanoblasts are also **migrating dorsolaterally**.

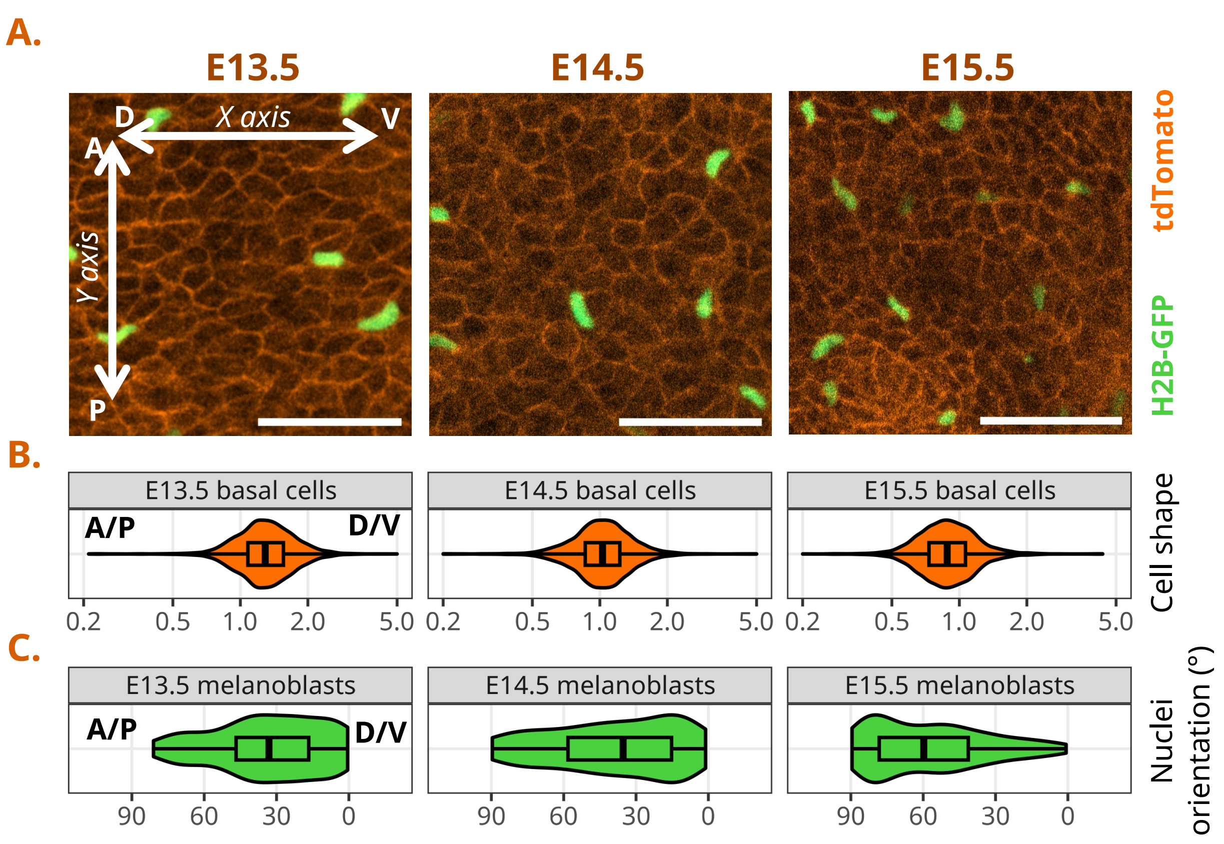

Fig 2: Morphologies of basal epidermis in whole iDct-G;mT embryos. A. Confocal slices of dorsal-most skin. Scale bars 50 µm. **B.** Basal cell shape, measured by aspect ratio (cell width/cell height). **C.** Melanoblast nuclei orientation, longest axis angle of elongated (circularity < 0.8) nuclei respective to X axis. D/V: dorsal/ventral, A/P: anterior/posterior.

Hypothesis: Anisotropic tension across the basal epidermis directs melanoblast migration.

Ex-vivo imaging under reproducibly applied force

- We developed a **stretch system** for controlled mechanical manipulation of **E13.5-E15.5** mouse embryonic skin.
- **Explants** are stretched and **live imaged** on deformable **PDMS** membranes[6] in a custom **incubated chamber**.

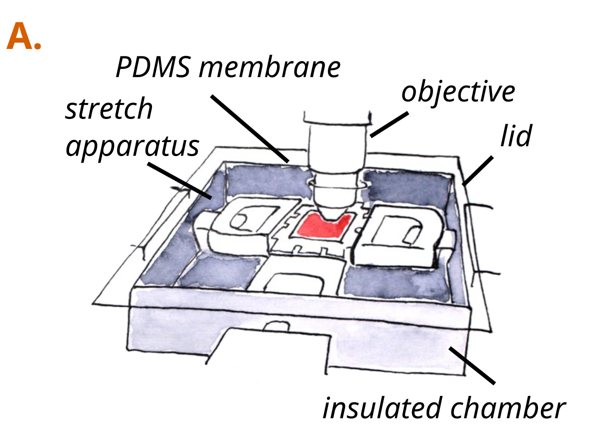

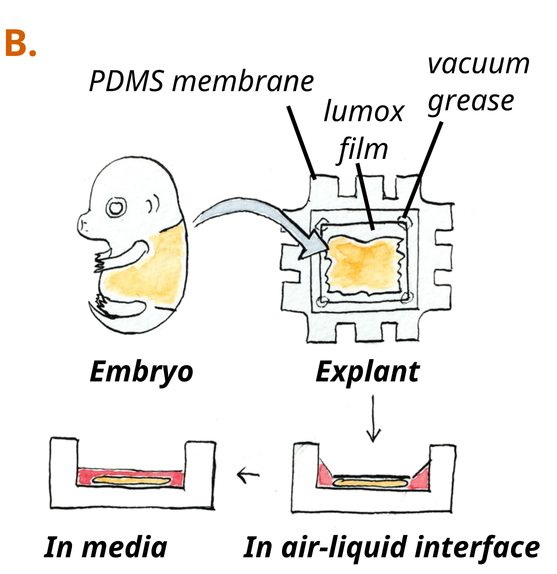

Fig 3: The "HATHA" stretch system. A. Diagram of system components. **B.** Diagram of the back skin dissection and PDMS membrane mount protocol.

Results

Dorsoventral stretch elongates basal epidermal cells

- We **timelapse imaged** dorsal regions of E14.5 explants 2 hrs pre- and 2 hrs post- application of **5.0 mm uniaxial** stretch across D/V (X) axis.
- This **induces** D/V elongation in basal epidermal cells:

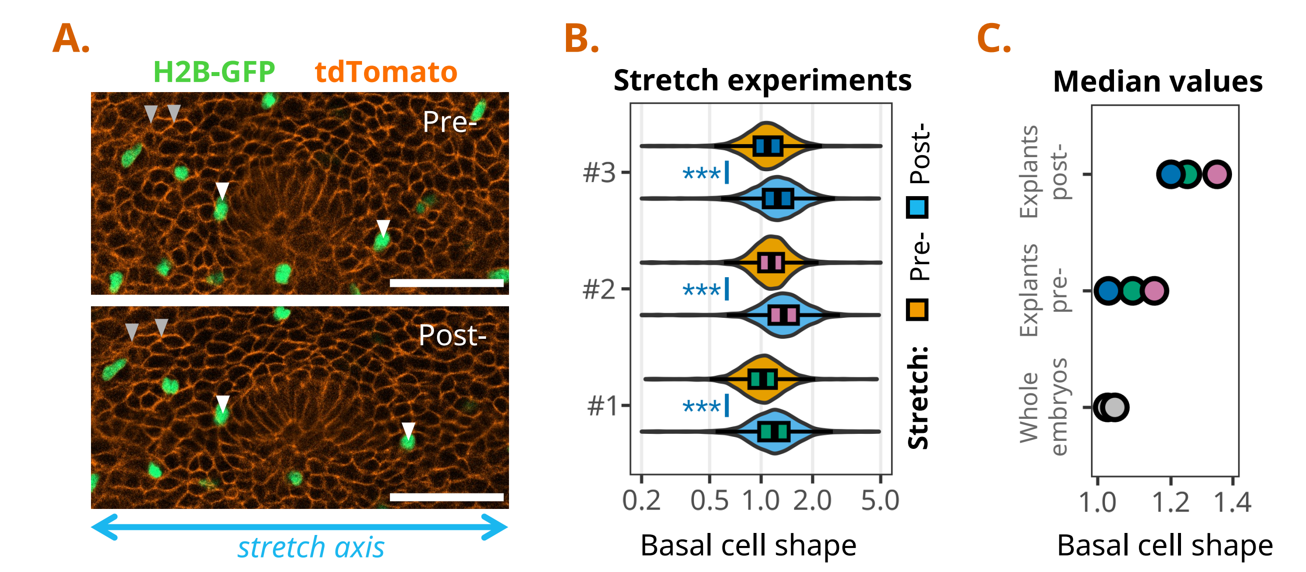

Fig 4: E14.5 iDct-G;mT basal epidermis pre- and post- 5 mm D/V stretch. A. Last frame of a pre-stretch and first frame of a post-stretch timelapse. Arrows indicate same basal cell edges (grey) and pair of melanoblasts (white). Scale bars 50 µm. **B.** Quantification of basal cell aspect ratios in 3 stretch experiments. *** = p<0.001, KS test. **C.** Median aspect ratios from 3 explants pre- or post- stretch compared to 2 whole embryos.

Movement and orientation of elongated melanoblast nuclei aligns with stretch axis

- 2D tracking of nuclei revealed that a greater population of melanoblasts are **migrating in the X direction** after stretch.
- In **elongated** nuclei, angles of displacement and longest shape axis **correlate** and both align **parallel** with stretch.

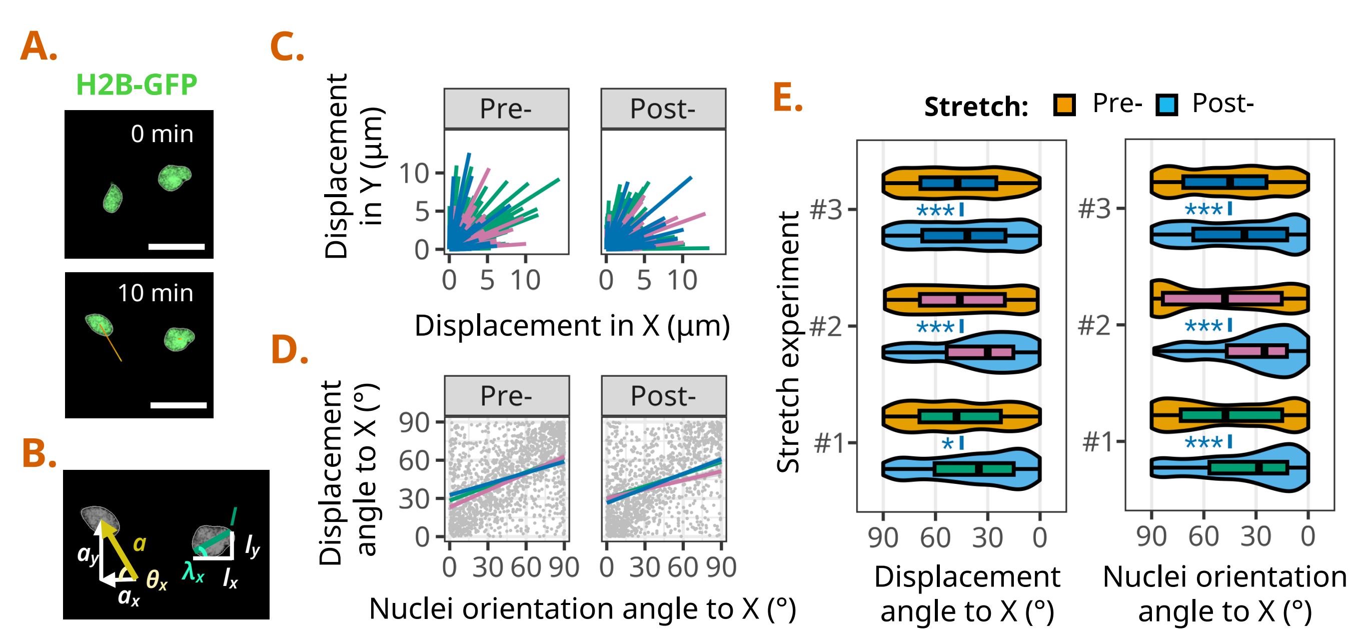

Fig 5: Tracking of E14.5 iDct-G;mT melanoblasts pre- and post- stretch. A. Successive frames of a sum intensity projected timelapse visualising melanoblast displacement vectors (orange). Scale bars 20 µm. **B.** Calculations of displacement angle θ and longest shape axis angle λ. **C.** Displacement vectors of elongated melanoblast nuclei (circularity < 0.8) plotted for 3 stretch experiments. **D.** Scatterplot of displacement and shape angles of elongated nuclei. Linear regressions plotted for each experiment, correlation tested by Spearman, p<0.001 for all plots. **E.** Movement and shape orientation of elongated nuclei in 3 stretch experiments. * = p<0.05, *** = p<0.001, KS test.

Axial trends of elongated nuclei orientation across explants are altered by stretch

- We **tilescan imaged entire explants** pre- and post- 5.0 mm D/V stretch. Orientation effects in elongated melanoblast nuclei were **replicated**.
- **Trends** in nuclear orientation were seen across both D/V and A/P axes. Stretch produced the strongest effect in the **dorsal-most** region, in the middle of the PDMS membrane.

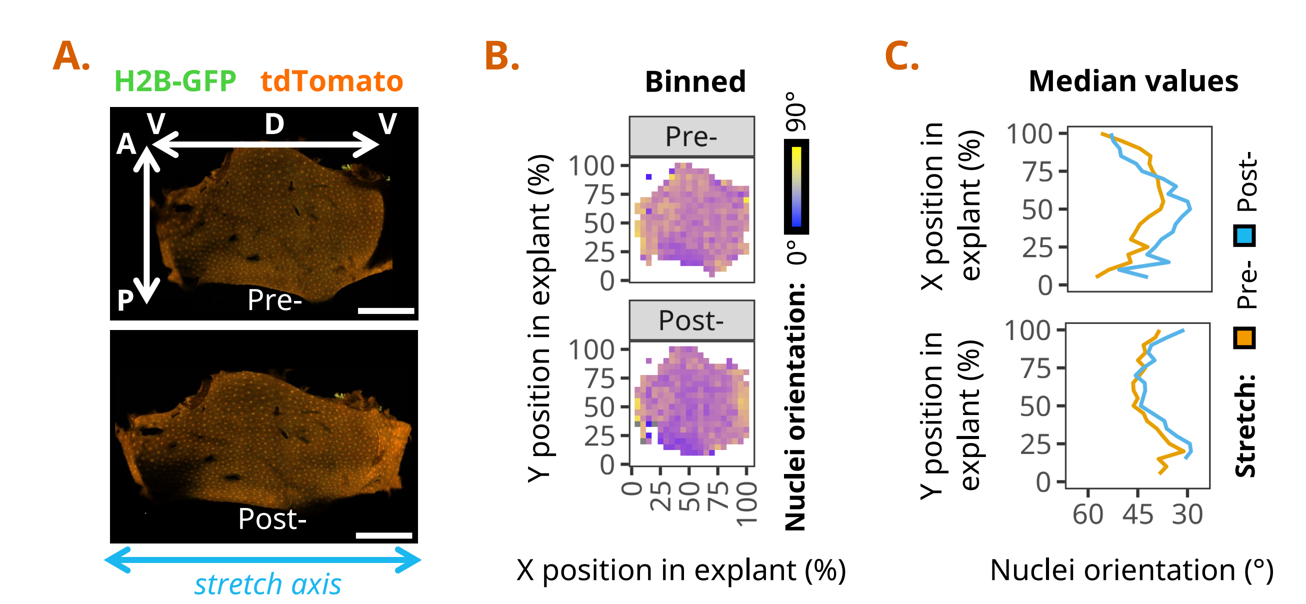

Fig 6: Mapping effects of D/V stretch in whole E14.5 iDct-G;mT explants. A. Sum intensity projections of tilescans of one sample. Scale bars 2 mm. **B.** Example of binning of explant data on a coordinate system, visualising representative regional trends of melanoblast nuclei orientation. **C.** Median nuclei orientation of 3 explants pre- and post- stretch across Y or X axis using the binned coordinates.

Future directions

- Evaluate how stretch across **anterior-posterior axis** affects melanoblast migration directionality.
- Use **laser ablation** to measure tension on epithelial cell edges pre- and post- stretch and compare this with intact embryos.
- Employ the **iDct-GT** mouse model – cross of iDct-GFP and Ai63[7] strains – to visualise **cell shapes and protrusions** of migrating melanoblasts under stretch.

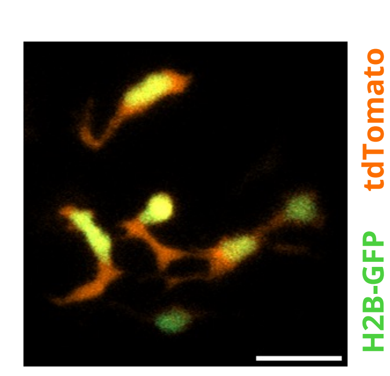

Fig 7: Epidermal melanoblasts of an E16.5 iDct-GT embryo. Sum intenisty projection, scale bar 20 µm.

References

1. Aw WY, et al. *Curr Biol.* 2016;26(16):2090-100.
2. Damen M, et al. *Nat Commun.* 2021;12(1):3227.
3. Villeneuve C, et al. *Nat Cell Biol.* 2024;26(2):207-18
4. Zaidi RM, et al. *Pigment Cell Melanoma Res.* 2011;24:393–4.
5. Muzumdar MD, et al. *Genesis.* 2007;45(9):593-605.
6. Goddard GK, et al. *Cold Spring Harb Protoc.* 2020;(3):105551.
7. Daigle TL, et al. *Cell*, 2018;174:465-480.